

Constraining the nuclear energy density functional with quantum Monte Carlo calculations

Alessandro Roggero,^{1,*} Abhishek Mukherjee,^{2,3} and Francesco Pederiva^{4,5}

¹*Institute for Nuclear Theory, University of Washington, Seattle, WA 98195, US*

²*ECT*, Villa Tambosi, I-38123 Villazzano (Trento), Italy*

³*ClusterVision B.V., Nieuw-Zeelandweg 15B, 1045 AL, Amsterdam, Netherland*

⁴*Physics Department, University of Trento, via Sommarive 14, I-38123 Trento, Italy*

⁵*INFN-TIFPA, Trento Institute for Fundamental Physics and Applications*

(Dated: September 27, 2018)

We study the problem of an impurity in fully polarized (spin-up) low density neutron matter with the help of an accurate quantum Monte Carlo method in conjunction with a realistic nucleon-nucleon interaction derived from chiral effective field theory at next-to-next-to-leading-order. Our calculations show that the behavior of the proton spin-down impurity is very similar to that of a polaron in a fully polarized unitary Fermi gas. We show that our results can be used to put tight constraints on the time-odd parts of the energy density functional, independent of the time-even parts, in the density regime relevant to neutron-rich nuclei and compact astrophysical objects such as neutron stars and supernovae.

Introduction.— The *ab initio* prediction of nuclear properties from quantum chromodynamics (QCD) remains an unresolved challenge in fundamental science. Its importance extends well beyond the confines of basic nuclear physics, into the realm of astrophysics, viz. in the physics of neutron stars and core-collapse supernovae.

It is unlikely that direct lattice QCD calculations of many hadron properties will be possible in the foreseeable future. However, in the past two decades a promising alternative route has been proposed and pursued with vigor. This scheme consists of bridging the gap between QCD and low energy nuclear physics by building successive effective theories.

In the first step one constructs an effective Hamiltonian with the hadronic degrees of freedom. The structure of this Hamiltonian is tightly constrained by chiral effective field theory (EFT) [1]. In the next stage one performs accurate many body calculations with this effective Hamiltonian for simple configurations, e.g. homogeneous matter, light and medium mass nuclei etc. Results from these calculations, in conjunction with experimental data, are eventually used to construct an energy density functional (EDF) for nuclear systems. Density functional theory is, presently, the only viable computational method for complex inhomogeneous systems.

It is of paramount importance that the effective theory at each stage is consistent with the available experimental data and the predictions of the underlying microscopic theory. A successful prototype is provided by the density functional theory for electronic structure calculations [2] which was fit to accurate quantum Monte Carlo (QMC) calculations for the electron gas [3]. Of course, nuclear systems are far more complicated because of the complexity of the nuclear forces and the remaining ambiguities in their short range structure.

Most nuclear EDFs are fit to the ground state properties of even-even nuclei, saturation properties of nuclear

matter and occasionally to microscopic calculations of unpolarized neutron matter. These quantities constrain only that part of the EDF which depends on the time-reversal-even densities (“time-even part”). The EDF also depends on time-reversal-odd densities (“time-odd part”) which plays an important role in a variety of phenomena: binding energies of odd-mass nuclei [4], pairing correlations in nuclei [5], distribution of the Gamow-Teller strength [6], properties of rotating nuclei [7], nuclear magnetism [8] etc. At present, the time-odd part of the Skyrme and other non-relativistic nuclear EDF is ill-determined because of the lack of unambiguous constraints from experiment or *ab-initio* calculations.

In the recent past, there is an emerging consensus that the theoretical uncertainties of the nuclear forces is largely suppressed in low density neutron matter (densities sufficiently less than the saturation density of nuclear matter). In this regime, the properties of the relevant components of the two nucleon forces are well established and the contributions from three and higher body forces are rather small. Any realistic nucleon-nucleon interaction, which fits the low energy nucleon-nucleon scattering phase shifts and the binding energy of deuteron, in conjunction with an accurate many body method produce consistent “theoretical data”; which can provide constraints for the EDF complementary to those coming from experiments.

In this paper we report the results from fully non-perturbative QMC calculations with a chiral EFT Hamiltonian for fully polarized (spin up) low density neutron matter with an impurity (spin down neutron or spin up/down proton). The impurity problem that we discuss here is a generalization of the well known polaron problem in solid state systems and in ultracold gases (see, e.g. in [9]). In fact, we find that the proton spin-down impurity behaves in a manner which is qualitatively very similar to a polaron in a fully polarized

Fermi gas in the unitary regime, i.e., the regime with diverging s-wave scattering length ($a_s \rightarrow \infty$) and vanishing effective range ($r_e \rightarrow 0$), over a wide density range $10^{-3} \text{ fm}^{-3} \leq \rho \leq 5 \times 10^{-2} \text{ fm}^{-3}$.

We show that the difference between energies of the proton spin up and spin down impurities depends only on the time-odd part of the EDF. Thus, our results provide stringent constraints for the time-odd part of the density functional, *independent of the time-even part*. The results presented here will provide valuable guidance in constructing EDFs in regimes relevant to neutron-rich nuclei, neutron star crusts and supernovae neutrinosphere.

Method.— Our calculations are based on the recently developed QMC method called the configuration interaction Monte Carlo (CIMC) method [10–12]. The CIMC method is based on filtering out an eigenstate Ψ_0 of the Hamiltonian H by repeated application of the propagator $\mathcal{P} = e^{-\tau(H-E_T)}$ on an initial state Ψ_I ,

$$|\Psi_0\rangle = \lim_{N_\tau \rightarrow \infty} \mathcal{P}^{N_\tau} |\Psi_I\rangle. \quad (1)$$

Here, E_T is an energy shift used to keep the norm of the wave function approximately constant, and τ is a finite step in ‘imaginary’ time $\tau = it$. The state, Ψ_0 , is the eigenstate with the lowest eigenvalue within the subset of states having non-zero overlaps with Ψ_I .

The application of the propagator is carried out stochastically. The main difference between the CIMC method and traditional continuum diffusion Monte Carlo methods is that in the CIMC method this stochastic projection is performed in Fock space (i.e. the basis is provided by the Slater determinants that can be constructed from a finite set of single particle (sp) basis states), as opposed to the coordinate space. As a result, non-local Hamiltonians do not pose any technical problems.

In this work, we use the sp basis given by eigenstates of momentum and the z components of spin and isospin. The calculations for fully polarized neutrons are performed in a box containing N spin-up neutrons. The impurity system contains an additional impurity particle. Periodic boundary conditions are imposed. The size of the box is given by the density, ρ , of the spin-up neutrons, $L^3 = N/\rho$. The finite size of the box implies that the sp states are restricted to a lattice in momentum space with a lattice constant $l = 2\pi/L$.

A finite sp basis is chosen by imposing a ‘basis cutoff’ k_{max} , so that only those sp states with $\mathbf{k}^2 \leq k_{\text{max}}^2$ are included. A sequence of calculations, with successively larger values of k_{max} , are performed till convergence is reached. We deem the calculations to have converged in k_{max} when the difference in the energies between the successive calculations are smaller than the statistical error (~ 10 KeV).

Sampling of new states can be performed under the condition that the matrix elements of the propagator,

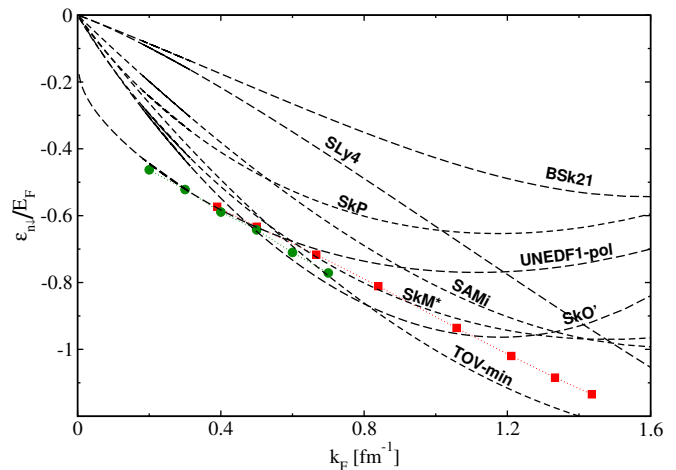


FIG. 1. (Color online) The energy of the neutron spin-down impurity in the units of the Fermi energy of the spin-up neutrons. The red filled squares are our QMC results with the NNLO_{opt} interaction. The green filled circles are the GFMC calculations with an s-wave interaction fit to the nm scattering length and effective range [14]. The black dashed lines are predictions from various density functionals (see text).

\mathcal{P} , are always positive semi-definite. For fermions interacting via realistic potentials, this condition is never fulfilled. (An interesting exception is provided by the pure pairing Hamiltonian [13].) This gives rise to the so-called sign-problem, which we circumvent by using a guiding wave function to constrain the random walk to a subsector of the full many-body Hilbert space in which the sampling procedure is well defined [10]. This restriction of the random walk introduces an approximation which is similar to the fixed-node/fixed-phase approximation commonly used in continuum QMC. Our method provides strict variational upper bounds for the energy.

As explained in Refs. 11 and 12, we use coupled cluster double (CCD) type wave functions as the guiding wave functions. As a result, the CIMC method provides an interesting synthesis of QMC methods and coupled cluster (CC) theory. In principle, the fixed phase approximation can be systematically improved by including irreducible triples, quadrupoles etc. in the guiding wave function. However, as discussed in Ref. 12 these contributions are expected to be rather small at these densities (less than a few percent of the total correlation energy).

Results.— We calculate the ground state energies for a fully polarized system and that with an additional impurity particle. The difference between these two energies gives the impurity energy. We use the recently developed next-to-next-to-leading order chiral NNLO_{opt} interaction [15] for our calculations. The scattering phase shifts obtained from this interaction fit the experimental database [16] at $\chi^2 \sim 1$ for laboratory energies less than 125 MeV. However, as alluded to in the introduction, the conclusions we present are *independent* of the particular inter-

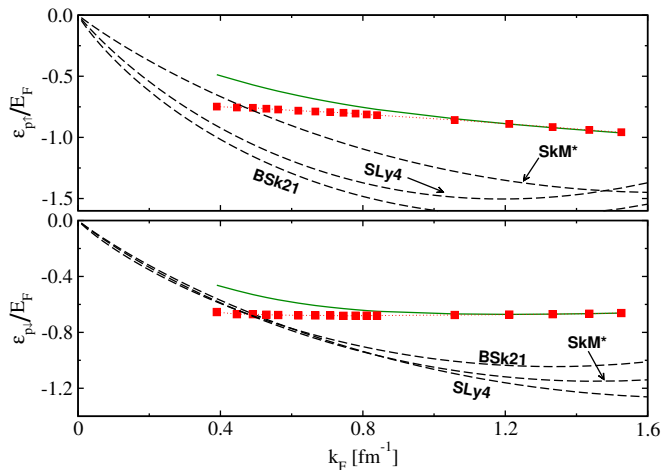


FIG. 2. (Color online) The energy of the proton spin-up (top panel) and spin-down (bottom panel) impurities in the units of the Fermi energy of the spin-up neutrons. The red filled squares are our QMC results with the NNLO_{opt} interaction. The green solid lines are the results from second order perturbation theory. The black dashed lines are predictions from various density functionals (see text).

action model we are using.

In Fig. 1 we plot the ratio of the energy of neutron spin-down impurity, $\varepsilon_{n\downarrow}$, and the Fermi energy of the fully polarized system, E_F , versus the Fermi momentum k_F . Our results are in good agreement with the GFMC calculations reported in Ref. 14 using an s -wave interaction (fit to the nn scattering length and effective range). For example, at $k_F = 0.4 \text{ fm}^{-1}$, we get $\varepsilon_{n\uparrow}/E_F = -0.582 \pm 0.002$ while the GFMC calculation gives -0.589 ± 0.005 . An AFDMC calculation performed the Argonne v'_8 potential gives -0.567 ± 0.006 at the same k_F .

The impurity energies reported in Fig. 1 and later in Fig. 2 were performed with $N = 7$ spin-up neutrons. We have checked in selected cases that the difference between the $N = 7$ and the $N = 33$ energies is about 1 – 2%. For example, for $\rho = 0.04 \text{ fm}^{-3}$ $\varepsilon_{n\downarrow}/E_F$ is -0.6698 ± 0.0005 with $N = 7$ and is -0.664 ± 0.006 for $N = 33$, while for $\rho = 0.06 \text{ fm}^{-3}$ the corresponding values are -0.6617 ± 0.0003 and -0.647 ± 0.004 . With $N = 7$ the size of the box, L , for the largest density we consider in this work ($\rho = 0.06 \text{ fm}^{-3}$) is about 4.9 fm. This is about three times the characteristic range of the nucleon-nucleon interaction given by the pion Compton wavelength ($\approx 1.4 \text{ fm}$). At higher densities ($\rho \geq 0.16 \text{ fm}^{-3}$) the corrections resulting from performing calculations with a finite number of particles is expected to be sizeable and it is customary to perform calculations with larger particle number ($N \geq 33$, for each spin). However, at the densities we are considering in this paper, the finite particle number corrections (even at $N = 7$) can be reasonably expected to be smaller than, or at most comparable to, the other sources of uncertainty (the non

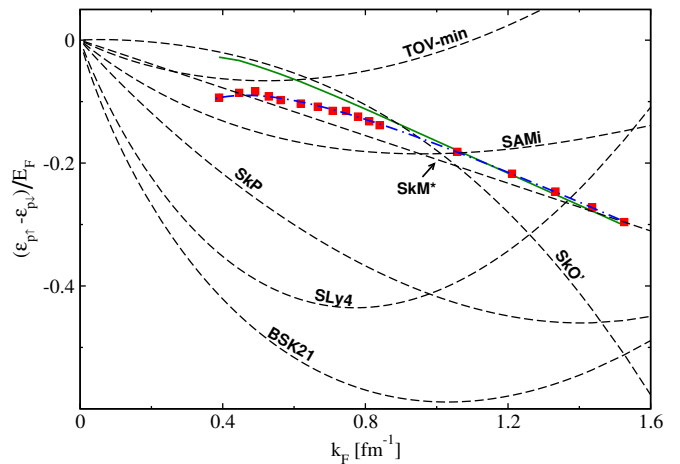


FIG. 3. (Color online) The difference between the energies of the proton spin-up and spin-down impurities in the units of the Fermi energy of the spin-up neutrons. The red filled squares are our QMC results with the chiral NNLO_{opt} interaction. The green solid line is the prediction from second order perturbation theory. The blue dot-dashed line is a fit of the form: $A - \frac{B}{k_F|a_s|} - Ck_F r_e$. The black dashed lines are predictions from various density functionals (see text).

inclusion of three body forces in the Hamiltonian or the absence of triples in the wave function).

In Fig. (2) we plot the ratio of the energy of the proton spin up/down impurity ($\varepsilon_{p\uparrow/\downarrow}$) and E_F . The density dependence of $\varepsilon_{p\uparrow/\downarrow}/E_F$ is rather weak. In fact, the QMC results for $\varepsilon_{p\downarrow}/E_F$ change by less than 2% ($-0.681 < \varepsilon_{p\downarrow}/E_F < -0.666$) when the density changes by more than an order of magnitude ($10^{-3} - 5 \times 10^{-2}$). Interestingly, this value is larger, in magnitude, than the corresponding (theoretical) value for polaron energy in a fully polarized unitary Fermi gas (≈ -0.6) [17] by about 10%. It is worth pointing out here that the singlet pn scattering length is about 25% larger than the singlet nn scattering length. This weak density dependence of $\varepsilon_{p\uparrow/\downarrow}$ is a non-perturbative result. Calculations from second order perturbation theory, also shown in the figure, predict a much stronger density dependence for $k_F < 1.0 \text{ fm}^{-1}$.

The Skyrme EDF for uniform matter is usually parametrized as

$$\mathcal{E} = \mathcal{E}_{\text{kin}} + \sum_{t=0,1} (C_t^p \rho_t^2 + C_t^T \rho_t \tau_t + C_t^s s_t^2 + C_t^T s_t T_t). \quad (2)$$

where \mathcal{E}_{kin} is the kinetic energy density. The isoscalar (isovector) density, spin-density, kinetic density and spin-kinetic density are denoted by ρ_0, s_0, τ_0 and T_0 (ρ_1, s_1, τ_1 and T_1), respectively. The part of the density functional which explicitly depends on the time-odd densities (s_t, T_t) is the time-odd part, and the rest is the time-even part.

The coefficients C_t^p, C_t^T, C_t^s and C_t^T can only depend on the total (isoscalar) density $\rho_0 = \rho$. In general, the coeffi-

coefficients are all independent and should be fixed from available data. However, for EDFs derived from a Skyrme force, there are additional relationships amongst the coefficients and the number of independent coefficients is smaller. Usually the C_t^p and C_t^s are assumed to have the form

$$C_t^{(\rho/s)} = C_t^{(\rho/s)0} + C_t^{(\rho/s)\rho} \rho^{(\gamma/\delta)}. \quad (3)$$

The impurity energy can be calculated from the EDF as

$$\varepsilon_{\tau\sigma} = \left. \frac{\partial \mathcal{E}}{\partial \rho_{\tau\sigma}} \right|_{\rho_{\tau\sigma} \rightarrow 0}, \quad (4)$$

with $\tau\sigma = \{n \downarrow, p \uparrow, p \downarrow\}$. In Fig. (1) we also show $\varepsilon_{n\downarrow}/E_F$ obtained from a wide cross-section of currently popular EDFs: SLy4 [18], SkM* [19], BSk21 [20], SkP [21], SkO' [22], SAMi [23], TOV-min [24] and UNEDF-pol [14]. In Fig. 2, we show $\varepsilon_{p\uparrow/\downarrow}/E_F$ for a smaller sub-section of the EDFs. This is done in order to avoid over-crowding the figure. However, we would like to note here that the three EDFs, which are plotted in Fig. 2, provide a fair representation of the spread in the predictions from the current Skyrme-type EDFs; all the other EDFs show very similar trends both qualitatively and quantitatively.

None of the EDFs reproduce the QMC results satisfactorily. This is even more evident in the case of the proton spin-down impurity; whereas all the EDFs predict $\varepsilon_{p\downarrow}/E_F$ to be decreasing with k_F , our QMC calculations predict a flat behavior. This is not unexpected since the EDFs are usually fit to the experimental properties nuclear systems near saturation density and low isospin polarization (stable nuclei), and many body calculations of unpolarized neutron matter. On the basis of our calculations we conclude that in order to account for the correlations in the low density matter in the presence of large spin and isospin polarization, *qualitative changes* are warranted in the form of the EDFs.

The difference $\varepsilon_{p\uparrow} - \varepsilon_{p\downarrow}$ is a purely time-odd quantity. From Eqs. (2) and (4) one can easily obtain the following relation

$$\frac{\varepsilon_{p\uparrow} - \varepsilon_{p\downarrow}}{E_F} = \frac{4m(C_0^s - C_1^s)}{3\pi^2\hbar^2} k_F - \frac{2m(C_0^T - C_1^T)}{5\pi^2\hbar^2} k_F^3. \quad (5)$$

In Fig.(3) we compare the predictions from our QMC calculations for $(\varepsilon_{p\uparrow} - \varepsilon_{p\downarrow})/E_F$ with those from different EDFs. It is clear that none of the EDFs correctly describe our results. The SkM* EDF reproduces the linear part of our results reasonably well. However, the SkM* EDF does not perform any better than the other EDFs for the individual $\varepsilon_{p\uparrow/\downarrow}$. Also, globally the SkM* EDF fares significantly worse than the more modern EDFs in describing experimental data for nuclei (e.g., masses).

Our results are well fit by the form

$$\frac{\varepsilon_{p\uparrow} - \varepsilon_{p\downarrow}}{E_F} = A - \frac{B}{k_F |a_s|} - C k_F r_e \quad (6)$$

with $A = 0.17 \pm 0.01$, $B = 1.4 \pm 0.1$ and $C = 0.101 \pm 0.001$. We have used the values $a_s = -23.75$ fm and $r_e = 2.75$ fm for the neutron-proton singlet scattering length and effective length, respectively. This form is clearly reminiscent of a dilute unitary Fermi gas.

Conclusion.— We have presented QMC calculations with a chiral interaction for the impurities in low density fully polarized neutron matter. The proton spin-down impurity shows universal behaviour for a wide range of densities. None of the state of the art Skyrme EDFs describe our microscopic calculations correctly. We showed that the difference between the proton impurity energies depends only on the time-odd part of the EDF. We found a simple functional form which fits our results for this difference, but is nevertheless qualitatively different from what is predicted by the current functional forms used in the Skyrme EDFs. Our results provide new constraints for constructing accurate density functionals.

Acknowledgments.— We thank A. Gezerlis for sharing the results of their numerical simulations. The authors are also members of LISC, the Interdisciplinary Laboratory for Computational Science, a joint venture between Fondazione Bruno Kessler and the University of Trento. Computations have been carried out mostly on the open facilities at Lawrence Livermore National Laboratory.

* roggero@uw.edu

- [1] E. Epelbaum, H. W. Hammer, and U. G. Meißner, Rev. Mod. Phys. **81**, 1773 (2009); R. Machleidt and D. R. Entem, Phys. Rep. **503**, 1 (2011); H. W. Hammer, A. Nogga, and A. Schwenk, Rev. Mod. Phys. **85**, 197 (2013).
- [2] J. P. Perdew and Y. Wang, Phys. Rev. B **45**, 13244 (1992).
- [3] D.M. Ceperley and B.J. Alder, Phys. Rev. Lett. **45**, 566 (1980).
- [4] W. Satula, in *Nuclear Structure'98, AIP Conf. Proc. No. 481 (AIP, New York, 1999)*, edited by C. Baktash, p. 114.
- [5] T. Duguet, P. Bonche, P. H. Heenen, and J. Meyer, Phys. Rev. C **65**, 014310 (2001).
- [6] M. Bender, J. Dobaczewski, J. Engel, and W. Nazarewicz, Phys. Rev. C **65**, 054322 (2002).
- [7] J. Dobaczewski and J. Dudek, Phys. Rev. C **52**, 1827 (1995); U. Post, E. Wüst, and U. Mosel, Nucl. Phys. **A437**, 274 (1985).
- [8] A. V. Afanasjev and P. Ring, Phys. Rev. C **62**, 031302 (2000).
- [9] F. Chevy and C. Mora, Rept. Prog. Phys. **73**, 112401 (2010); P. Massignan, M. Zaccanti, and G. M. Bruun, Reports on Progress in Physics **77**, 034401 (2014).
- [10] A. Mukherjee and Y. Alhassid, Phys. Rev. A **88**, 053622 (2013).
- [11] A. Roggero, A. Mukherjee, and F. Pederiva, Phys. Rev. B **88**, 115138 (2013).
- [12] A. Roggero, A. Mukherjee, and F. Pederiva, Phys. Rev. Lett. **112**, 221103 (2014), arXiv:1402.1576 [nucl-th].

- [13] N. Cerf and O. Martin, Phys. Rev. C **47**, 2610 (1993); A. Mukherjee, Y. Alhassid, and G.F. Bertsch, *ibid.* **83**, 014319 (2011).
- [14] M.M. Forbes, A. Gezerlis, K. Hebeler, T. Lesinski, and A. Schwenk, Phys. Rev. C **89**, 041301(R) (2014).
- [15] A. Ekström, G. Baardsen, C. Forssén, G. Hagen, M. Hjorth-Jensen, G. R. Jansen, R. Machleidt, W. Nazarewicz, T. Papenbrock, J. Sarich, and S. M. Wild, Phys. Rev. Lett. **110**, 192502 (2013).
- [16] V. G. J. Stoks, R. A. M. Klomp, M. C. M. Rentmeester, and J. J. de Swart, Phys. Rev. C **48**, 792 (1993).
- [17] C. Lobo, A. Recati, S. Giorgini, and S. Stringari, Phys. Rev. Lett. **97**, 200403 (2006); N. Prokof'ev and B. Svistunov, Phys. Rev. B **77**, 020408 (2008).
- [18] E. Chabanat, P. Bonche, P. Haensel, J. Meyer, and R. Schaeffer, Physica Scripta **1995**, 231 (1995); Nucl. Phys. **A627**, 710 (1997); **A635**, 231 (1998).
- [19] J. Bartel, P. Quentin, M. Brack, C. Guet, and H.-B. Håkansson, Nucl. Phys. **A386**, 79 (1982).
- [20] S. Goriely, N. Chamel, and J.M. Pearson, Phys. Rev. C **82**, 035804 (2010).
- [21] J. Dobaczewski, H. Flocard, and J. Treiner, Nucl. Phys. **A422**, 103 (1984).
- [22] P. G. Reinhard, D. J. Dean, W. Nazarewicz, J. Dobaczewski, J. A. Maruhn, and M. R. Strayer, Phys. Rev. C **60**, 014316 (1999).
- [23] X. Roca-Maza, G. Colo, and H. Sagawa, Physical Review C **86**, 031306 (2012).
- [24] J. Erler, C.J. Horowitz, W. Nazarewicz, M. Rafalski, and P.-G. Reinhard, Phys. Rev. C **87**, 044320 (2013).